Kilohertz-Linewidth Brillouin Photonic Crystal Fiber Laser With Non-Resonance Pumping Configuration

Guoqing Ji, Zhiyuan Huang, Wenbin He, Ruochen Yin, Yu Zheng, Xin Jiang, Yuxin Leng, and Meng Pang

***Abstract*—Brillouin fiber laser with the non-resonance pumping configuration, has compact set-up, good wavelength tunability and high-power single-frequency-emission capability, being regarded as an important technique for highly-coherent light generation. Such Brillouin fiber lasers, using single-mode fiber (SMF) as the Brillouin gain medium, generally have high lasing thresholds and mode-hopping instabilities, resulting from the relatively-low Brillouin gain coefficient of the conventional SMF. Here, we report a compact, non-resonance-pumping Brillouin photonic crystal fiber laser that can generate kHz-level-linewidth single-frequency lasing with tens-of-mW lasing threshold. Mode-hopping instability of this laser is largely suppressed thanks to the short (∼20 m) cavity length, which gives rise to a free-spectral-range (FSR) value of ∼10 MHz properly matching the tens-of-MHz Brillouin gain bandwidth. Experimental results of both self-heterodyne and frequency-noise measurements indicate a laser linewidth of ∼1.4 kHz, corresponding to high linewidth-narrowing ratio of ∼18. No lasing line of high-order Stokes was observed in experiments as the laser pump power was gradually increased to ∼200 mW, giving a nearly-linear lasing slope.**

***Index Terms*—Brillouin scattering, photonics crystal fiber, fiber laser.**

Manuscript received 9 March 2024; revised 25 April 2024; accepted 4 May 2024. Date of publication 9 May 2024; date of current version 21 May 2024. This work was supported in part by the National Natural Science Foundation of China under Grant 62275254, Grant 62205353, and Grant 62375275, in part by National High-level Talent Youth Project, Shanghai Science and Technology Innovation Action Plan under Grant 21ZR1482700, in part by the Strategic Priority Research Program of the Chinese Academy of Science under Grant XDB0650000, in part by Shanghai Science and Technology Plan Project Funding under Grant 23JC1410100, in part by Key R&D Plan of Ningbo City under Grant 2023Z105, and in part by Fuyang High-level Talent Group Project. *(Guoqing Ji and Zhiyuan Huang contributed equally to this work.) (Corresponding authors: Wenbin He; Meng Pang.)*

Guoqing Ji is with the State Key Laboratory of High Field Laser Physics and CAS Center for Excellence in Ultra-intense Laser Science, Shanghai Institute of Optics and Fine Mechanics (SIOM), Chinese Academy of Sciences (CAS), Shanghai 201800, China, and also with the Center of Materials Science and Optoelectronics Engineering, University of Chinese Academy of Sciences, Beijing 100049, China.

Zhiyuan Huang is with the State Key Laboratory of High Field Laser Physics and CAS Center for Excellence in Ultra-intense Laser Science, Shanghai Institute of Optics and Fine Mechanics (SIOM), Chinese Academy of Sciences (CAS), Shanghai 201800, China, and also with the Russell Centre for Advanced Lightwave Science, Shanghai Institute of Optics and Fine Mechanics and Hangzhou Institute of Optics and Fine Mechanics, Hangzhou 311421, China.

Wenbin He and Xin Jiang are with the Russell Centre for Advanced Lightwave Science, Shanghai Institute of Optics and Fine Mechanics and Hangzhou Institute of Optics and Fine Mechanics, Hangzhou 311421, China (e-mail: wenbin.he@r-cals.com).

Ruochen Yin is with the Russell Centre for Advanced Lightwave Science, Shanghai Institute of Optics and Fine Mechanics and Hangzhou Institute of Optics and Fine Mechanics, Hangzhou 311421, China, and also with iFiber Optoelectronics Technology Company Ltd., Ningbo 315105, China.

Yu Zheng is with iFiber Optoelectronics Technology Company Ltd., Ningbo 315105, China.

Yuxin Leng is with the State Key Laboratory of High Field Laser Physics and CAS Center for Excellence in Ultra-intense Laser Science, Shanghai Institute of Optics and Fine Mechanics (SIOM), Chinese Academy of Sciences (CAS), Shanghai 201800, China.

Meng Pang is with the State Key Laboratory of High Field Laser Physics and CAS Center for Excellence in Ultra-intense Laser Science, Shanghai Institute of Optics and Fine Mechanics (SIOM), Chinese Academy of Sciences (CAS), Shanghai 201800, China, and also with the Russell Centre for Advanced Lightwave Science, Shanghai Institute of Optics and Fine Mechanics and Hangzhou Institute of Optics and Fine Mechanics, Hangzhou 311421, China (e-mail: pangmeng@siom.ac.cn).

Digital Object Identifier 10.1109/JPHOT.2024.3399030

I. Introduction

HIGH-PERFORMANCE single-frequency lasers with high spectral purities and therefore low frequency noise levels, are of great demand in coherent optical telecommunications [1], optical ranging and lidar [2], distributed fiber sensing [3], optical gyroscope [4], [5] and microwave synthesizer [6], [7]. While commercial single-frequency lasers based on semiconductor technique have normally MHz or sub-MHz linewidths, linewidth narrowing of these lasers using stimulated Brillouin scattering (SBS), especially in optical fibers [3], [4], [6], [8], [9], [10], [11], [12] or planar waveguides [5], [7], [13], [14], has been at the focus of attention for many years.

Brillouin lasers could be generically divided into two catalogues according to their pumping configurations: resonance and non-resonance pumping, as illustrated in Fig. 1. In the resonance-pumping scheme, the frequency of the pump light should be locked tightly with one longitudinal mode of the laser cavity (see Fig. 1(a)), which can efficiently enhance the pump intensity inside the cavity with a high finesse [8], [9], [13], [14]. Such enhancement due to resonance can largely decrease the lasing threshold of the laser, and the additional work is to set the cavity length or free spectral range (FSR) to match with the Brillouin frequency shift, so as to ensure that another longitudinal cavity mode lying within the narrow Brillouin gain band, see Fig. 1(a). While this resonance-pumping configuration brings a few advantages such as low lasing threshold and high linewidth-narrowing ratio [15], the locking between the pump frequency and the cavity resonance restricts, to some extent, the compactness as well as the frequency-tuning ability of the Brillouin fiber laser (BFL). Moreover, due to the simultaneous operation of both the clockwise and counter-clockwise resonances (see Fig. 1(a)), it is more challenging for this resonance-pumping configuration to suppress cascaded lasing at high-order Stokes lines, especially at high pump powers [11], [13].

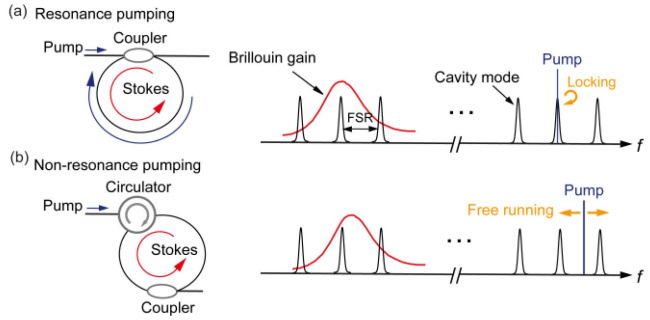

Fig. 1. Conceptual illustration of Brillouin lasers with resonance pumping (a) and non-resonance pumping (b) configurations.

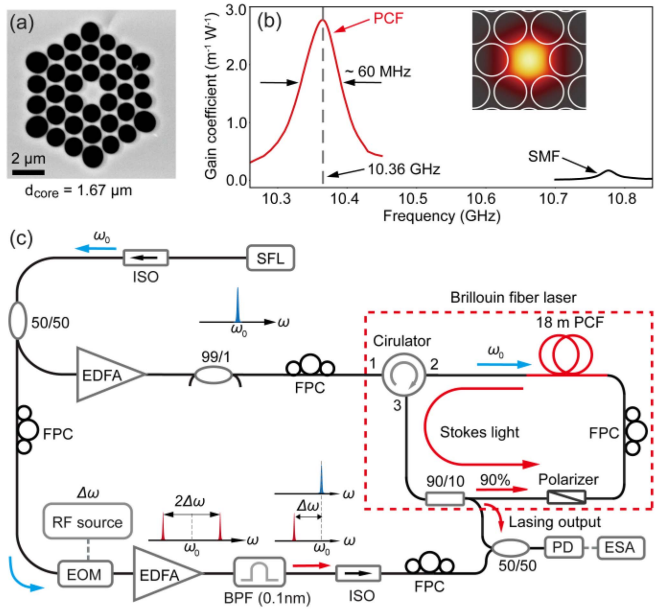

Fig. 2. (a) SEM photograph of PCF sample used in the laser set-up. (b) Measured Brillouin gain spectrum of the PCF. The simulated fundamental mode profile in the PCF core is illustrated as the inset. (c) Experimental set-up of both the Brillouin fiber laser (BFL) and the heterodyne measurement. SFL, single frequency laser; EDFA, erbium-doped fiber amplifier; FPC, fiber polarization controller; EOM, electric-optic modulator; BPF, band-pass filter; ISO, isolator; PD, photodetector; ESA, electric spectrum analyzer.

An alternative scheme of Brillouin lasing is the non-resonance-pumping configuration [10], [12], [16], [17], [18], [19], as conceptually illustrated in Fig. 1(b). The use of an optical circulator provides isolation of the clockwise pump light, while forming a laser cavity for only the counter-clockwise Stokes light. This single-pass layout of the pump light releases the locking requirement for the pump laser frequency (see Fig. 1(b)), however it increases largely the lasing threshold [10], [12]. For example, Wang *et.al* demonstrated a Brillouin fiber laser using 10-m-long single mode fiber (SMF) as the gain medium, the lasing threshold of this Brillouin laser is ∼920 mW [12], mainly due to the relatively-low Brillouin gain coefficient of the SMF. Even though the use of longer (hundreds of meters) Brillouin gain fiber can efficiently lower the Brillouin lasing threshold, it would lead to small cavity FSR and therefore mode-hopping instability. Additional stabilization mechanism, based on optical filter [16] or phase-locking electronics [17], could be used to suppress this mode-hopping effect, which, however, increases the system complexity. Some previous studies demonstrated that chalcogenide fiber [18] and waveguides [19], with much higher nonlinearity coefficients than SMF, could be used to provide high Brillouin gain in short lengths. The use of chalcogenide materials results in, however, some difficulties in the low-loss integration of the laser system, and the relatively-low damage threshold of chalcogenide materials (compared to silica glass) limits the laser power scaling.

The small-core, silica photonic crystal fiber (PCF) can provide high optical nonlinearity due to its μm-sized core diameter, giving rise to a large Brillouin gain coefficient more than ten times higher than that of the conventional SMF [20], [21], [22]. The enhanced Brillouin gain of the small-core PCF could largely decrease the lasing threshold, especially for the non-resonance-pumping configuration. Additionally, the advanced splicing technique between the PCF and SMF [23] makes the all-in-fiber laser set-up possible. In this work, we demonstrate a prototype Brillouin photonic crystal fiber laser that can deliver kHz-level single-frequency output using a compact laser set-up, with moderate lasing threshold and less mode-hopping instability. The 18-m-long PCF sample used in the experiment had a small core diameter of ∼1.7 μm, corresponding to a Brillouin gain coefficient that is ∼16 times higher than that of conventional SMF [22]. The use of the small-core, highly-nonlinear PCF decreases largely the lasing threshold of the Brillouin laser, and the resulting short cavity length gives rise to a cavity FSR comparable to the Brillouin gain bandwidth of the PCF, efficiently suppressing mode-hopping instability of the laser. The non-resonance pumping scheme together with the all-silica-fiber configuration renders this Brillouin fiber laser great power-scaling capability, avoiding completely cascaded Brillouin lasing at high-order Stokes lines.

II. Experimental Set-Up

The scanning electron microscope (SEM) photo of the PCF sample used in the Brillouin fiber laser is illustrated in Fig. 2(a), and its Brillouin gain spectrum in Fig. 2(b), was measured using the pump-probe method [22]. The Brillouin gain spectrum of a section of conventional SMF was also measured using the same method and the results are plotted in Fig. 2(b) for a direct comparison. The PCF sample exhibits a Brillouin frequency shift of 10.36 GHz and a Brillouin gain bandwidth of ∼60 MHz. Compared to SMF, ∼16 times enhancement of the Brillouin gain coefficient is mainly due to much smaller mode area of the PCF, and the difference of Brillouin frequency shift between the PCF and SMF results mainly from the fact that the fundamental optical mode of the PCF has a smaller refractive index value (∼1.4) than that (∼1.45) of the SMF [22]. To construct the Brillouin fiber laser set-up, a single-frequency semiconductor laser (CTL1550 from Toptica) at ∼1550 nm, with an output power of 18 mW and a central frequency of $\omega_0$was used to provide the seed light. After passing through an optical isolator and a 50/50

coupler, see Fig. 2(c), this seed laser was boosted by an Er-doped fiber amplifier (EDFA, AEDFA-27-B-FA from Amonics). The output from the EDFA was then launched into the circulator as the pump light of the Brillouin laser, after passing through in sequence of a 99/1 coupler for pump-power monitoring and a fiber polarization controller (FPC) for pump-polarization-state adjustment.

In the Brillouin laser cavity, the 18-m-long PCF sample was fusing spliced with SMF using short (∼1 cm) samples of transition fiber (UHNA7 fiber from Nufern) to bridge the large mode-area difference between the PCF and SMF [23]. In the experiment, we used a commercial fusion splicer (87S from Fujikura) to perform the fiber splicing and both the fusion current and fusion time have been manually adjusted to make the splicing loss as small as possible. Typical splicing loss between the SMF and the UNHA fiber is ∼0.4 dB, while the loss between UNHA7 and PCF is ∼2 dB. Therefore, the total insertion loss of the PCF sample, including a SMF-UNHA7-PCF port and a PCF-UNHA7-SMF port, is typically ∼5 dB. Inside the cavity, a polarizer was used to ensure the polarized Stokes-light generation. Please note that even though the Stokes light at the output port of the polarizer is linearly-polarized, over propagation in SMF or PCF the polarization state of light would change due to some intrinsic birefringence of the fiber. However, such variation in polarization state will not degrade the degree of polarization (light components at two orthogonal polarization states remain to be coherent). In the experiment, a polarization controller could be used at the output port of the laser, which can transform a polarized light beam (with any polarization state) to linearly-polarized light.

A FPC was also placed in the laser cavity, just before the PCF sample, and it was used to adjust the polarization state of the Stokes light. In the experiment, we adjusted simultaneously this intra-cavity FPC and the FPC before the optical circulator, see Fig. 2(c), to vary simultaneously the polarization states of both the pump and Stokes light beams. By doing this, we could maximize the laser output power and to minimize the lasing threshold. A 90/10 coupler was used to provide the laser output. The total cavity loss was estimated to be ∼8 dB.

The total cavity length is ∼20 m, giving rise to a cavity FSR of ∼11 MHz. The cavity FSR is a bit narrower than the Brillouin gain bandwidth (∼60 MHz) of the PCF. Nevertheless, stable single-longitude-mode operation of this Brillouin fiber laser can be observed in the experiment, see our results below. The single-frequency operation can be attributed to the fact that the ∼11 MHz mode-spacing can lead to enough discrepancy of the Brillouin gain coefficients at different longitude modes. Additionally, when the laser is operating, the PCF should provide a Brillouin gain of ∼8 dB to compensate the cavity loss. This will lead to the gain narrowing effect expressed as: $G(f) = \exp[g(f)P_{\mathrm{pump}}L]$, where $G(f)$ is the exact Brillouin gain in the PCF, $g(f)$ is the Brillouin gain coefficient of the fiber, P_{pump} is laser pump power and L is the PCF length. This gain narrowing effect could further increase the discrepancy of Brillouin gain values at different longitude modes.

In order to characterize the spectral property of the Brillouin laser output, a heterodyne set-up [24] was constructed in the experiment, see Fig. 2(c). A portion of seed light was modulated using an electro-optical modulator (EOM), generating two sideband components with a frequency difference of $2\Delta\omega$. The modulation signal was generated using a radio-frequency (RF) source whose modulation frequency ($\Delta\omega$) can be precisely tuned over a broad span from 100 MHz to 20 GHz, with Hz-level resolution. The output light from the modulator was amplified using an EDFA (AEDFA-PA-35-FA from Amonics) and the low-frequency component was filtered out using a tunable optical filter (WTF-200-T01-1550-SMF from Alnair labs) with a narrow bandwidth of 0.1 nm. At a modulation frequency of ∼10 GHz, the frequency difference between the two components is ∼20 GHz, which corresponds to a wavelength difference of ∼0.16 nm at 1550 nm. Therefore the 0.1-nm-bandwidth optical filter can provide reasonably-good suppression to the high-frequency component. The filtered lower-frequency component, after passing through an optical isolator and a FPC, was launched into a 50/50 coupler, mixing with the Brillouin laser output. Two FPCs were used in this heterodyne set-up. While the first FPC before the EOM was used to adjust the polarization state of light to match the principal axis of the modulator, the second FPC before the 50/50 coupler was used to adjust the polarization state of the amplified light to ensure a high signal-to-noise ratio of the beating signal. The heterodyne signal was then detected by a photodetector (PD, PDB450C from Thorlabs) and analyzed by an electrical spectrum analyzer (ESA, N9030B from Keysight).

III. Lasing Threshold Measurements

In the experiment, when we gradually increased the pump power of the Brillouin fiber laser, clear transition features of both the laser output power and the laser linewidth were observed at the 10% port of the 90/10 coupler, see Fig. 3(a) and (b), indicating a Brillouin lasing threshold of ∼90 mW. The laser output power was measured at the output coupler using a power meter. Below the lasing threshold, the laser linewidth was measured using the heterodyne set-up, see Fig. 2(c). Above the threshold, the narrow linewidth of the Brillouin fiber laser was measured using the self-heterodyne set-up, see Fig. 5(a). As can be seen in Fig. 3(b), below the lasing threshold, the laser output is the spontaneous Brillouin scattering light which has a linewidth of several tens of MHz, a sharp linewidth narrowing to a few kHz has been observed at pump powers above the lasing threshold.

At a pump power of 154 mW, the laser output power was measured to be ∼2.8 mW, corresponding to a Stokes light power of ∼76 mW generated in the PCF. At this pump level, we measured the laser output spectrum and the pump light spectrum with an optical spectrum analyzer (OSA, AQ6370D from Yokogawa with 0.01 nm resolution). The results are illustrated in Fig. 3(c). The wavelength difference (0.09 nm) between the pump and Stokes light agrees well with the Brillouin frequency shift of the PCF sample (10.36 GHz).

As illustrated in Fig. 3(a), the output power of this Brillouin fiber laser is ∼4 mW at a pump power of 180 mW, corresponding to a lasing efficiency of merely 2.2%. The lasing slope efficiency was estimated to be ∼4.2%, see Fig. 3(a). The relatively-low lasing efficiency is mainly due to the low (10%) ratio of the output coupler as well as the high insertion loss of the PCF sample. In practice, the laser output power could be increased to

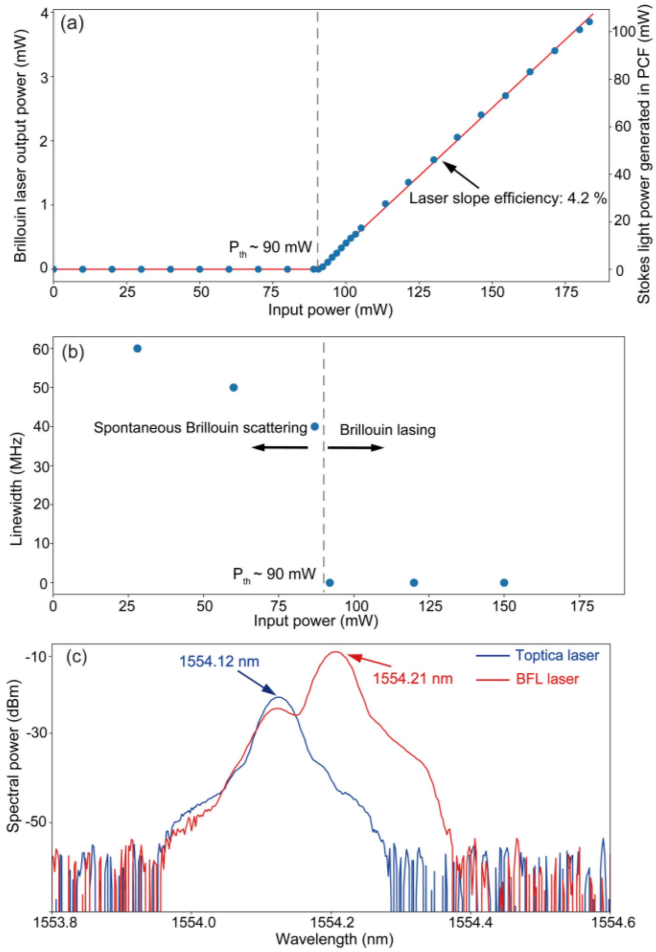

Fig. 3. (a) Output power of the Brillouin fiber laser as the function of the pump power, giving a laser slope efficiency of 4.2%. (b) Measured linewidths of the laser output light at different pump powers. 60 MHz at 28 mW pump power, 50 MHz at 60 mW, 40 MHz at 87 mW, 1.72 kHz at 92 mW, 1.32 kHz at 120 mW, and 1.30 kHz at 150 mW. (c) Optical spectra of the pump and the Brillouin lasers, measured using an OSA.

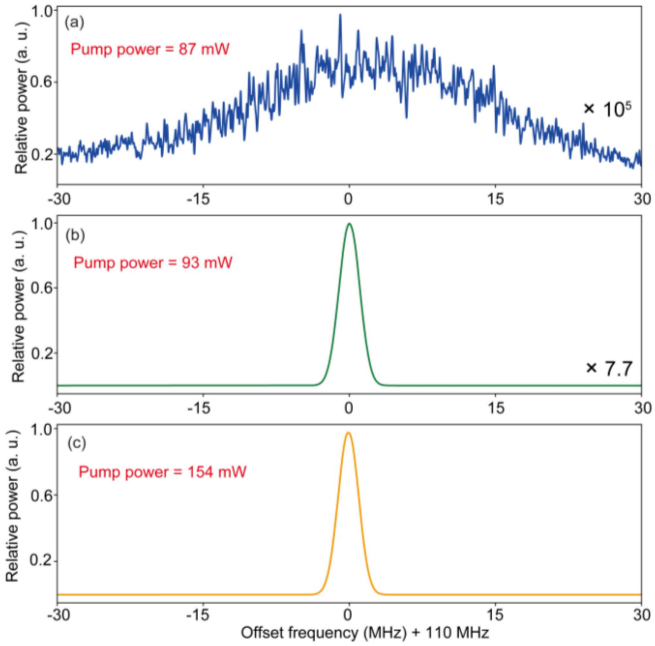

Fig. 4. Beating signal of the heterodyne measurement at pump powers of (a) 87 mW (below the lasing threshold) and (b) 93 mW and (c) 154 mW (above the threshold). Abrupt narrowing of the laser linewidth was obtained just above the lasing threshold. The signal traces of (a) and (b) were amplified by 100000 times and 7.7 times, respectively.

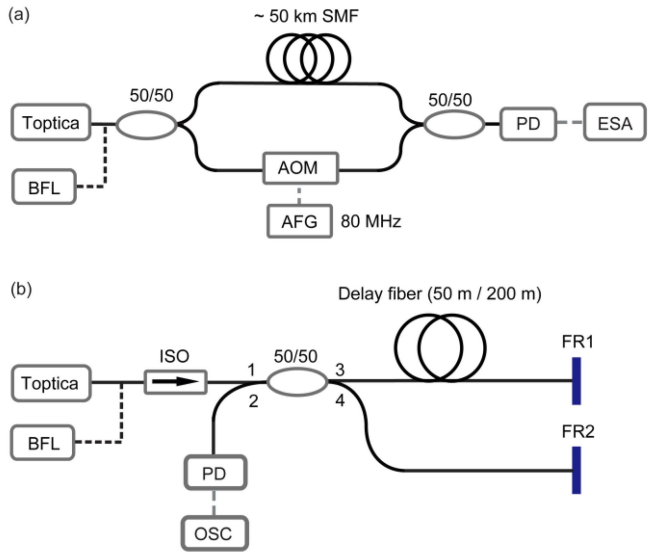

Fig. 5. Diagnostic set-ups for the self-heterodyne detection measurement (a) and the frequency-noise measurement (b).

~10 mW simply through using a 30/70 output coupler, which would also lead to a slight increase of the lasing threshold. At a pump power of 180 mW, we can estimate the power of the Brillouin Stokes light generated in the PCF sample is ~101 mW, giving a stimulated Brillouin scattering efficiency of ~56% in the PCF.

As illustrated in Fig. 3(c), the optical signal-to-noise ratio (OSNR) of this Brillouin fiber laser was measured to be >50 dB, which we think is mainly limited by the noise floor of the optical spectrum analyzer used in the experiment. In principle, the OSNR level of the Brillouin fiber laser is closely related to the noise performance of the pump laser [15] and the OSNR noise performance of this laser is worth in-depth investigation in future studies.

The heterodyne traces measured at three different pump powers of 87 mW (below the lasing threshold), 93 mW and 154 mW (above the lasing threshold) were illustrated in Fig. 4. Below the lasing threshold, the typical heterodyne trace corresponds to the beating signal between the modulated pump light and the ultra-weak (sub-pW level) spontaneous Brillouin scattering light form the PCF, as illustrated in Fig. 4(a). At a pump power of 87 mW, the spontaneous Brillouin scattering light exhibits a linewidth of ~40 MHz (close to the Brillouin gain bandwidth), see Fig. 4(a). At higher pump powers (above the threshold), sudden linewidth narrowing from ~40 MHz to ~1 MHz was observed, see Fig. 4(b) and (c). The ~1 MHz linewidth in these measurements was mainly limited by the scanning resolution of the ESA.

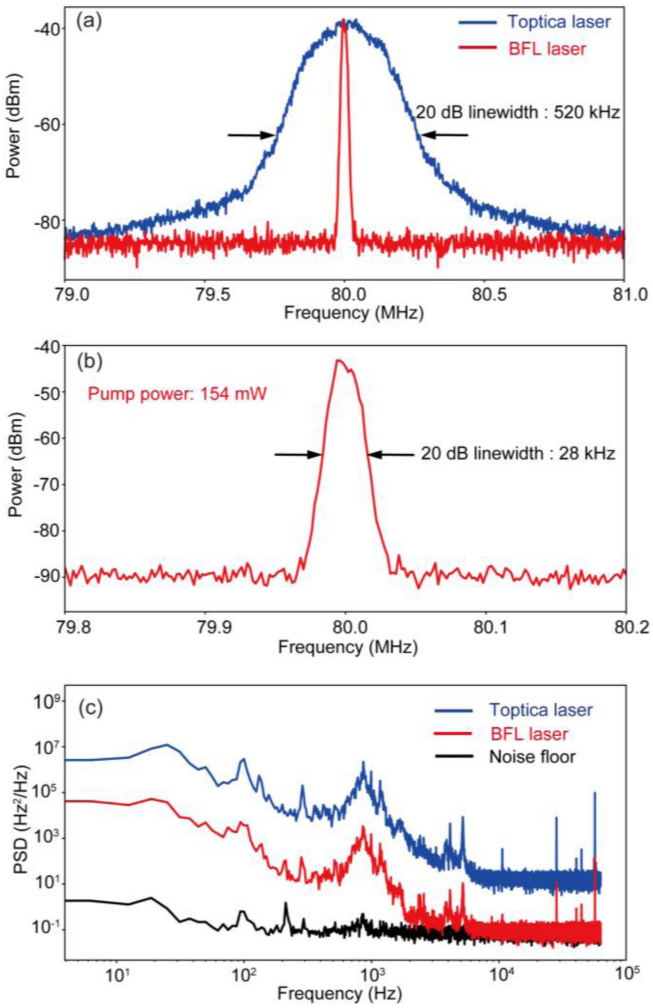

Fig. 6. (a) and (b) Measured self-heterodyne signal for the pump laser (blue curve) and the Brillouin fiber laser (red curve). The settings of the ESA during these measurements are: center frequency: 80 MHz, frequency span: 2 MHz/ 400 kHz, resolution: 1.0 kHz. (c) Power spectral density of the measured frequency noise for the pump laser (blue curve) and the Brillouin fiber laser (red curve). The noise floor of the measurement is also plotted as the black curve.

IV. Linewidth and Frequency-Noise Measurements

In order to characterize precisely the coherence performance of the Brillouin fiber laser, two diagnostic set-ups were constructed (see Fig. 5) to perform separately self-heterodyne and frequency-noise measurements. In the self-heterodyne measurement, the laser output under test was split into two paths by a 50/50 coupler. While an acousto-optic modulator (AOM) was used in one path with a modulation frequency of 80 MHz, the 50-km-long SMF was used in the other path as the delay fiber, ensuring the incoherent combination of the light beams at the second 50/50 coupler [25], see Fig. 5(a). Then, the beating signal from the coupler was detected by the photodetector and the ESA. Using this self-heterodyne set-up, the linewidths of both the pump laser and the Brillouin fiber laser were measured, when the self-heterodyne set-up was put in a soundproof box to avoid environmental perturbations. As illustrated in Fig. 6(a) and (b), the 20-dB linewidth of the pump laser was measured to be 520 mW (a 3-dB linewidth 26 kHz), and the 20-dB linewidth of the Brillouin fiber laser to be 28 kHz (a 3-dB linewidth of 1.4 kHz), giving rise to a high linewidth narrowing ratio (defined as the pump laser linewidth divided by the lasing linewidth) of ∼18. Note that as illustrated in Fig. 3(c), the Brillouin laser output contains residual pump-frequency component which could result from the Rayleigh scattering of the pump light in the PCF and tiny back-reflected pump light by the fiber devices inside the laser cavity. In the experiment, we didn't use any optical filter when performing self-heterodyne measurements. This is because that the power level of the residual pump light is ∼18 dB lower than the Stokes light, and therefore the beating signal of the residual pump light is ∼36 dB lower than that of the Stokes lasing light in the self-heterodyne measurement, which would make trivial influence on the linewidth measurement of the Brillouin fiber laser.

Frequency noise measurements of both lasers were performed using an imbalanced Michaelson interferometer [25], [26], see Fig. 5(b). When the fiber interferometer operates at its quadrature point, the delay fiber in one arm of the interferometer can be used to transfer the laser frequency noise (Δf) to intensity noise (ΔI) at the interferometer output [25], which is described as:

$$\Delta I = \frac{2\pi I_0 \Delta L}{c} \Delta f \tag{1}$$

where I_0 is the light intensity in one arm, $\Delta L$the length of delay fiber, and c the speed of light. In the experiment, we measured the frequency noise of the pump laser using a delay-fiber length of 50 m, and the measured noise spectrum is plotted as the blue curve in Fig. 6(c). The frequency noise spectrum of the Brillouin fiber laser was measured using a delay-fiber length of 200 m, and the result is plotted as the red curve for comparison. A reduction of the noise power spectral density (PSD), by more than 20 dB, can be obtained for the Brillouin fiber laser, see Fig. 6(c). Through integrating these PSDs over a frequency range of 50 Hz to 60 kHz, we can estimate the integrated linewidths of the pump and Brillouin lasers to be 26.9 kHz and 1.5 kHz, respectively.

V. Discussion and Conclusion

In the experiment, we used PCF samples with different lengths as gain medium of the Brillouin laser and found that the lasing threshold increased gradually when we shortened the PCF length. For example, at a PCF length of 10 m, the cavity FSR increased to ∼17 MHz and the lasing threshold increased to ∼160 mW. For this 10-m-long PCF laser, the typical lasing linewidth was measured to be ∼1.9 kHz, and the performance of the laser single-mode stability, at PCF lengths of 10 m and 18 m, is quite similar. In the experiment, we did observe sometimes the longitudinal-mode-hopping phenomenon at this Brillouin fiber laser output, even though it has been largely suppressed thanks to the relatively-large cavity FSR [17] and the frequency pulling effect owing to strong dispersion in the Brillouin cavity [27]. We found in the experiment that mode-hopping instability of the laser happened every several minutes if the laser cavity was placed in a conventional optical laboratory, and its stability could

be further improved if the whole laser cavity was placed into a sound-proof box with a constant temperature.

For a fixed Brillouin laser configuration, the linewidth-narrowing ratio would be maintained in principle [15]. Therefore, the linewidth of the laser output is highly dependent on the linewidth of its pump laser. In the experiment, we used a kHz-level single-frequency laser (from NKT Photonics) to pump the same Brillouin laser set-up and observed a narrow-linewidth ($<$100 Hz, we estimated) output. However, it is difficult to measure accurately a laser linewidth of $<$100 Hz using the current self-heterodyne set-up [26]. A single-frequency laser with $<$100 Hz linewidth has a coherent length of $>$500 km, and such a long fiber delay would lead to unacceptable loss in the self-heterodyne set-up.

Moreover, the lasing threshold of this Brillouin fiber laser could be reduced through decreasing the laser cavity loss, which, in the current system, is mainly limited by the high insertion-loss of the PCF. Through optimizing both the PCF structure (for example, increasing slightly the PCF core size and decreasing the air-filling fraction in the PCF cladding) and the PCF splicing procedure, the pumping efficiency of the laser could be improved, and the Brillouin gain required for lasing could be reduced, both of which will lead to threshold reduction of this Brillouin photonic crystal fiber laser.

In conclusion, we report a compact, kHz-linewidth Brillouin fiber laser based on high-gain solid-core PCF. Spectral narrowing ratio as high as $\sim$18 was obtained in this non-resonance-pumping system with a moderate lasing threshold of $\sim$90 mW, and mode-hopping instability of this laser has been largely suppressed. The laser system demonstrated here may have some application potentials in distributed fiber sensing and optical ranging.

References

[1] E. Ip, A. P. T. Lau, D. J. F. Barros, and J. M. Kahn, "Coherent detection in optical fiber systems," *Opt. Exp.*, vol. 16, pp. 753–791, 2008.

[2] C. J. Karlsson, F. Å. A. Olsson, D. Letalick, and M. Harris, "All-fiber multifunction continuous-wave coherent laser radar at 1.55 μm for range, speed, vibration, and wind measurements," *Appl. Opt.*, vol. 39, pp. 3716–3726, 2000.

[3] A. A. Fotiadi, D. A. Korobko, and I. O. Zolotovskii, "Brillouin Lasers and Sensors: Trends and possibilities," *Optoelectron., Instrum. Data Process.*, vol. 59, pp. 66–76, 2023.

[4] F. Zarinetchi, S. P. Smith, and S. Ezekiel, "Stimulated Brillouin fiber-optic laser gyroscope," *Opt. Lett.*, vol. 16, pp. 229–231, 1991.

[5] J. Li, M.-G. Suh, and K. Vahala, "Microresonator Brillouin gyroscope," *Optica*, vol. 4, pp. 346–348, 2017.

[6] S. Molin, G. Baili, M. Alouini, D. Dolfi, and J. P. Huignard, "Experimental investigation of relative intensity noise in Brillouin fiber ring lasers for microwave photonics applications," *Opt. Lett.*, vol. 33, pp. 1681–1683, 2008.

[7] J. Li, H. Lee, and K. Vahala, "Microwave synthesizer using an on-chip Brillouin oscillator," *Nature Commun.*, vol. 4, 2013, Art. no. 2097.

[8] S. P. Smith, F. Zarinetchi, and S. Ezekiel, "Narrow-linewidth stimulated Brillouin fiber laser and applications," *Opt. Lett.*, vol. 16, pp. 393–395, 1991.

[9] J. Geng, S. Staines, Z. Wang, J. Zong, M. Blake, and S. Jiang, "Highly stable low-noise Brillouin fiber laser with ultranarrow spectral linewidth," *IEEE Photon. Technol. Lett.*, vol. 18, no. 17, pp. 1813–1815, Sep. 2006.

[10] G. Bashan, H. H. Diamandi, E. Zehavi, K. Sharma, Y. London, and A. Zadok, "A forward Brillouin fibre laser," *Nature Commun.*, vol. 13, 2022, Art. no. 3554.

[11] H. Ahmad, N. F. Razak, M. Z. Zulkifli, F. D. Muhammad, Y. Munajat, and S. W. Harun, "Ultra-narrow linewidth single longitudinal mode Brillouin fiber ring laser using highly nonlinear fiber," *Laser Phys. Lett.*, vol. 10, 2013, Art. no. 105105.

[12] G. Wang et al., "Watt-level ultrahigh-optical signal-to-noise ratio single-longitudinal-mode tunable Brillouin fiber laser," *Opt. Lett.*, vol. 38, pp. 19–21, 2013.

[13] S. Gundavarapu et al., "Sub-hertz fundamental linewidth photonic integrated Brillouin laser," *Nature Photon.*, vol. 13, pp. 60–67, 2019.

[14] W. Loh et al., "Dual-microcavity narrow-linewidth Brillouin laser," *Optica*, vol. 2, pp. 225–232, 2015.

[15] A. Debut, R. Stéphane, and Z. Jaouad, "Linewidth narrowing in Brillouin lasers: Theoretical analysis," *Phys. Rev. A*, vol. 62, 2000, Art. no. 023803.

[16] Z. Ou, X. Bao, Y. Li, B. Saxena, and L. Chen, "Ultranarrow linewidth Brillouin fiber laser," *IEEE Photon. Technol. Lett.*, vol. 26, no. 20, pp. 2058–2061, Oct. 2014.

[17] G. Danion et al., "Mode-hopping suppression in long Brillouin fiber laser with non-resonant pumping," *Opt. Lett.*, vol. 41, pp. 2362–2365, 2016.

[18] K. H. Tow et al., "Relative intensity noise and frequency noise of a compact Brillouin laser made of As38Se62 suspended-core chalcogenide fiber," *Opt. Lett.*, vol. 37, pp. 1157–1159, 2012.

[19] I. V. Kabakova et al., "Narrow linewidth Brillouin laser based on chalcogenide photonic chip," *Opt. Lett.*, vol. 38, pp. 3208–3211, 2013.

[20] J. H. Lee, Z. Yusoff, W. Belardi, M. Ibsen, T. Monro, and D. Richardson, "Investigation of Brillouin effects in small-core holey optical fiber: Lasing and scattering," *Opt. Lett.*, vol. 27, pp. 927–929, 2002.

[21] M. Merklein, I. V. Kabakova, A. Zarifi, and B. J. Eggleton, "100 years of Brillouin scattering: Historical and future perspectives," *Appl. Phys. Rev.*, vol. 9, 2022, Art. no. 041306.

[22] G. Ji et al., "Experimental studies on the core-structure dependence of backward Brillouin gain in solid-core photonic crystal fibers," *Opt. Exp.*, vol. 31, pp. 35742–35753, 2023.

[23] L. Xiao, M. Demokan, W. Jin, Y. Wang, and C. Zhao, "Fusion splicing photonic crystal fibers and conventional single-mode fibers: Microhole collapse effect," *J. Lightw. Technol.*, vol. 25, no. 11, pp. 3563–3574, Nov. 2007.

[24] L. B. Mercer, "1/f frequency noise effects on self-heterodyne linewidth measurements," *J. Lightw. Technol.*, vol. 9, no. 4, pp. 485–493, Apr. 1991.

[25] M. Pang, X. Bao, L. Chen, Z. Qin, Y. Lu, and P. Lu, "Frequency stabilized coherent Brillouin random fiber laser: Theory and experiments," *Opt. Exp.*, vol. 21, pp. 27155–27168, 2013.

[26] C. Spiefelberg, J. Geng, Y. Hu. Kaneda, S. Jiang, and N. Peyghambarian, "Low-noise narrow-linewidth Fiber laser at 1550 nm," *J. Lightw. Technol.*, vol. 22, no. 1, pp. 57–62, Jan. 2004.

[27] P.-A. Nicati, K. Toyama, S. Huang, and H. J. Shaw, "Frequency pulling in a Brillouin fiber ring laser," *IEEE Photon. Technol. Lett.*, vol. 6, no. 7, pp. 801–803, Jul. 1994.